24th INTERNATIONAL CONGRESS ON SOUND AND VIBRATION
23–27 July 2017, London

A CASE STUDY OF THRUST VARIATION FORCE DUE TO COUPLED TORSIONAL·AXIAL VIBRATION ON TWO STROKE LOW SPEED DIESEL ENGINES

Don Chool Lee

Mokpo National Maritime University, Jeollanam-do, Mokpo, South Korea
email: ldcvib@mmu.ac.kr

Sang-Hoon Kim

Mokpo National Maritime University, Jeollanam-do, Mokpo, South Korea

Ronald D Barro

Mokpo National Maritime University, Jeollanam-do, Mokpo, South Korea,

Marine propulsion shafting system propelled either by modern super large two-stroke low speed engines or by engines exploiting higher stroke/bore ratios typically operates at lower speed range (mcr). Consequently, this results in better propulsive efficiency and higher thrust variation force as well. The thrust variation force due to axial and torsional vibration occurring on the propulsion shafting system is transmitted to the engine and ship structure via thrust bearing. This force may manifest as engine body vibration or ship super structure vibration in a longitudinal direction and can reduce the crankshaft fatigue strength by additional stress in the crankshaft pin and journal along with torsional vibration. Additionally, actual thrust variation force measurement is difficult to perform.

In this paper, the axial vibration of propulsion shafting system with seven cylinder 7G80ME (24,400 kW@66 r/min) ultra-long stroke diesel engine and a fourteen cylinder 14RT-flex96C (80,080 kW@102 r/min) super-large diesel engine is ascertained by theoretical analysis and actual measurement. Both engines are installed with an axial damper of damping function and detuner of stiffness function respectively. Subsequently, the thrust variation force is estimated through this intermediate shaft axial amplitude on measurement and by correlating the thrust bearing stiffness and angular acceleration due to torsional vibration.

Keywords: thrust variation force, torsional vibration, axial vibration

Nomenclature

a_o	:	angular displacement amplitude
A_{xx1}	:	reaction force coefficient caused by propeller axial velocity
A_{xx2}	:	reaction force coefficient caused by propeller axial acceleration
B_{xx1}	:	reaction force coefficient caused by propeller angular velocity (torsion)
B_{xx2}	:	reaction force coefficient caused by propeller angular acceleration
D	:	propeller diameter
F_c	:	thrust variation force generated by propeller angular velocity
F_m	:	radial force due to torsional vibration
F_s	:	thrust variation force generated by the propeller angular acceleration
F_{torc}	:	crankshaft thrust force due to torsional vibration
F_{torp}	:	propeller thrust force due to torsional vibration
k	:	cylinder explosion order coefficient
K_L	:	dynamic stiffness for propeller axial direction
m, m_c, m_p	:	propeller mass, crank throw rotational mass, piston reciprocating mass
n, N_c	:	vibration order, number of cylinders

r, x_p, X_p	:	rotation radius of crank, propeller axial displacement, piston vertical displacement
P_a	:	axial force acting on crank journal
P_r	:	radial force acting on the crankpin
$[M]$, $\{X\}$	:	mass matrix, axial amplitude vector
$[C]$, $\{F_{ai}\}$	:	damping matrix, excitation force vector
$[K]$	:	stiffness matrix
γ, ω	:	phase angle, angular velocity
θ, $\emptyset$	:	crank throw rotation angle, connecting rod angle
λ (r/l), δ	:	connecting rod ratio, crankshaft axial displacement
α	:	phase angle of torsional vibration angular displacement
ρ	:	seawater density

1. Introduction

Green engines are super large-sized low-speed two-stroke engine with a higher number of cylinders and were developed to propel huge container vessels with the perceived benefit of increased propeller efficiency. The thrust force generated by the torsional and axial vibration by these engines is being transmitted to the hull through the thrust bearing. This results in an excitation force causing the longitudinal vibration on the upper hull portion. In addition for these large engines with higher number of cylinders, the increase in axial vibration along with the cylinder explosive forces will generate higher bending stresses on the crankshaft and becomes a factor decreasing the fatigue strength of the same propulsion shafting system. In this study, a 14RT-flex96C engine for a large container vessel and a 7G80ME engine for a super large tanker vessel were used as study model in the dynamic analysis of axial vibration through theoretical calculation and actual vibration measurement.

2. Axial vibration

2.1 Thrust force due to cylinder combustion pressure and torsional vibration

Marine diesel engine longitudinal vibration force can be calculated by considering first the force generated by the cylinder gas pressure and the inertial force due to the reciprocating mass of the crank pin. The reciprocating mass tangential force is divided into axial and radial direction. The constant tangential force can be regarded as the driving power of the engine while the deviating force acts as the excitation force causing the torsional vibration. In Fig. 1(A), the force acting on the right side bearing is fixed to be in the axial direction and it can be assumed to be translated radially in the axial direction as shown in Fig. 1(B) and this force becomes the excitation force of the axial vibration.

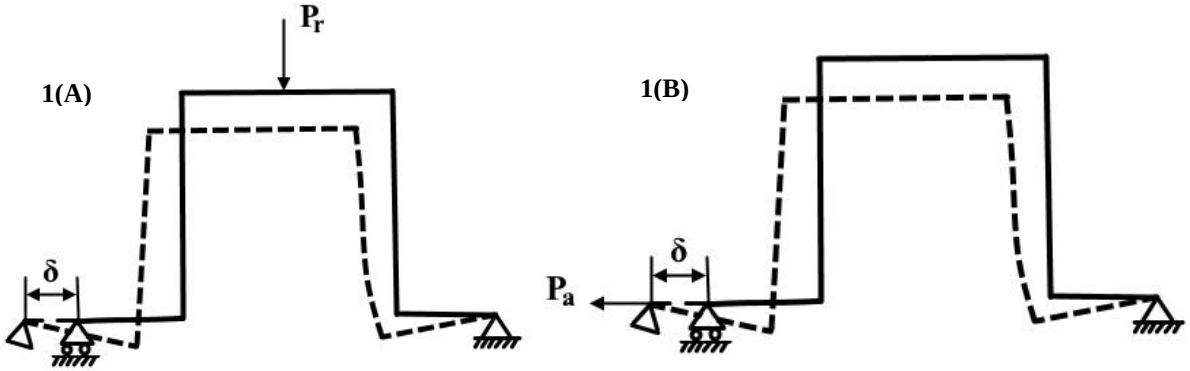

Figure 1: Conversion of radial force to axial force

Direct computation through complex modelling like FEM analysis may be possible but requires a lot of time and effort hence a simplified calculation is required for more convenient application. In terms of displacements, the radial force acting on the crankpin (P_r) can be considered as the force to

cause displacement in the axial direction on the journal and as function of the axial force required resulting for the crank throw (P_a) to displace in the axial direction as well. The thrust conversion ratio (η) value can be presumed depending on the adjacent angle of the crank throw, cylinder number and diameter, and the engine type. Though there is a slight difference in its value and considering the author's experience, the value can be given between 0.10 and 0.25. The axial force conversion rate (η) can be obtained as shown in Equation (1) and multiplying with the radial force acting on the crankpin (P_r), the excitation force of the axial vibration acting on the crank journal (P_a) is identified.

$$\eta = P_a/P_r \tag{1}$$

Secondly, if the excitation torque frequency coincides with the shafting system's natural frequency, torsional vibration stress also increases. As such, thrust variation occurs resulting to an increased axial displacement. The thrust force generated by the crank throw and the piston mechanism as shown in Fig. 2 due to torsional vibration is theoretically analysed and the force in radial direction is given as Eq. (2) [1].

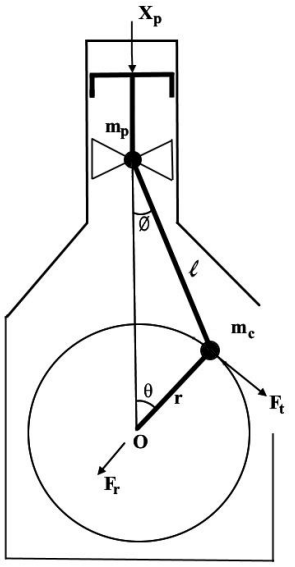

Figure 2: Inertia force of crank and piston

$$F_r = m_p\ddot{X}_p\{cos(\theta + \phi)/cos\phi\} - m_c r\dot{\theta}^2 \tag{2}$$

Expanding Eq. (2) and Eq. (3) is derived.

$$\begin{aligned} F_r = &-\{m_c + (m_p/2)r\dot{\theta^2}\} \\ &-(m_p/2)r\dot{\theta}^2\{\cos(2\theta) + (1/2\lambda)(\cos\theta + 3\cos(3\theta))\} \\ &-(m_p/2)r\ddot{\theta}\{\sin 2\theta + (1/\lambda)\,(-\sin\theta + \sin(3\theta))\} \end{aligned} \tag{3}$$

Here, assuming each respective amplitude of torsional vibration (a_o), the angular displacement (θ) can be expressed as Eq. (4).

$$\theta = \omega t + a_o \sin(n\omega t + \alpha) + (2\pi/N_c)k \tag{4}$$

Substituting Eq. (4) into Eq. (3)3 and taking into account the corresponding order only, Eqs. (5) and (6) is obtained.

$$F_m = \{m_c + m_p/2\}2nr\omega^2 a_o \sin\{n\omega t + \alpha + (\pi/2)\} \quad (5)$$

$$F_{torc} = \eta \cdot F_m \quad (6)$$

2.2 Thrust force generated by the propeller

Thrust variation force on the propeller caused by torsional vibrations can be calculated by theoretical analysis of the force acting on each part of the propeller. Although it can be applied, the calculation process is complicated and will require experts in this field to obtain more objectivity. Thereby, the data obtained from propeller models in experiment tanks were employed in this paper instead of the theoretical aspect [2]. Fig. 3 shows the impact coefficients for each propeller direction in respect to the three directions of the propeller respectively. Here, only the element (*x*-direction) directly influencing the longitudinal vibration is selected and the equations are obtained as given in Eqs. (7) and (8).

$$m\ddot{x}_p + K_L x_p = A_{xx2}\ddot{x}_p + A_{xx1}\dot{x}_p + B_{xx2}\ddot{\theta}_p + B_{xx1}\dot{\theta}_p \quad (7)$$

$$(m - A_{xx2})\ddot{x}_p - A_{xx1}\ddot{x}_p + K_L x_p = B_{xx2}\ddot{\theta}_p + B_{xx1}\dot{\theta}_p \quad (8)$$

If Eq. (4) is differentiated corresponding to the propeller and θ_p is substituted into the right-hand side of Eq. (8), the thrust force variation of the propeller (F_{torp}) can be expressed by Eq. (9).

$$F_{torp} = \sqrt{F_s^2 + F_c^2}\sin\{\alpha + \gamma + (\pi/2)\}$$
$$F_s = -B_{xx2}\rho D^4 n^2\omega^2 a_o, \quad F_c = 2B_{xx1}\rho D^4 n\omega^2 a_o$$
$$r = tan^{-1}(F_c/F_s) \quad (9)$$

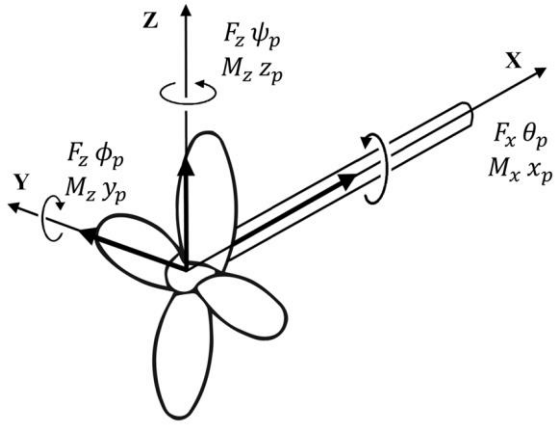

Figure 3: Direction of the reaction moments and displacements on the propeller

3. Theoretical Analysis

In order to calculate the axial vibrations of a marine diesel engine, it can be summarized as a general vibration equation as shown in Eq. (10).

$$[M]\{\ddot{X}\} + [C]\{\dot{X}\} + [K]\{X\} = \{F_{ai}\} \quad (10)$$

A 14RT-flex96C-B engine for a very large container vessel and a 7G80ME engine for a large oil tanker vessel were selected as study Model A and Model B and their mass – spring system is described in Fig. 4 respectively. The engine, dampers and propeller specifications are shown in Table 1. The cylinder was modelled assuming as one concentrated mass and the theoretical analysis was performed by dividing it into three mass systems per cylinder as Model B. In order to calculate the natural frequency and vibration mode of free vibration, it can be obtained by ignoring the attenuation and excitation force. The natural frequencies were calculated without damper and with a de-

tuner assumed to be rigid (attenuation x ω) and the results are given in Table 2. The forced vibration was obtained by using the transfer matrix method considering the nonlinearity of axial vibration damper whereas the forced vibration calculation is performed using the transfer matrix method. The axial amplitudes at the thrust bearing of the two model engines are shown in Fig. 5 [3].

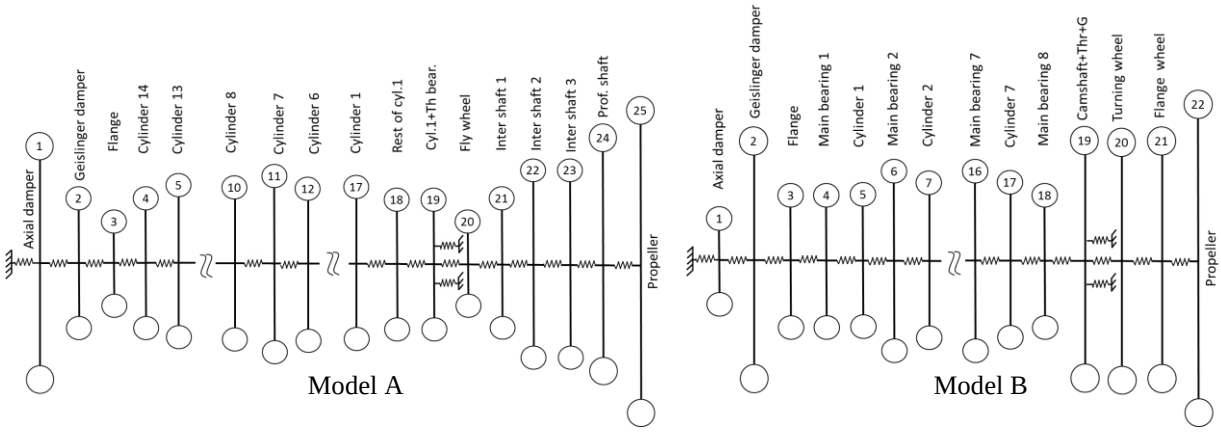

Figure 4: The mass – spring system model for subject engines

Table 1: Specification of Model A and Model B propulsion engine

Description		Units	Model A	Model B
Axial damper	Stiffness of thrust	MN/m	400	900
	Rel. damping	MN/s	--	1.0
	Weight	kg	4,200	6,200
Torsional damper	Type	---	Tuned D290/9	Tuned D325/1/V/M
	Diameter × Width	mm	3,300×190	3,250×Unknown
	Outer/Inner inertia	kg. m^2	18,700/1,640	26,600/2,600
	Stiffness	MN. m/rad	106	12.5
	Relative damping	kN-m/s	530.0	320.0
	Weight	kg	15,000	21,200
Main engine	Type	---	14RT-flex96C-B	7G80ME
	Cylinder bore × stroke	mm	900×2,500	800×3,720
	Power at MCR	kW × r/min	80,080×102	24,400×66
	Pmi at full load	bar	19.8	18.12
	Nominal torque	kN·m	4,000	3,530
	Reciprocating mass	kg/cylinder	17,384	14,161
	Firing order	---	1-8-14-9-2-5-10-12-7-3-4-13-11-6 (Uneven)	1-7-2-5-4-3-6
	Dia.(outer/inner) of crank shaft	mm	960/150	1010/0
	Conn. ratio	r/l	0.434	0.5
	No. of cylinder	---	14	7
	Weight	ton	2,300	1,055
Propeller	Type	---	Fixed pitch	Fixed pitch
	Diameter	m	9.0	10.6
	No. of blade (ea)	---	6	4
	Moment of inertia	ton. m^2 (in water)	663.45	449.85
	Weight	ton	105.3	71.37

Table 2: Natural frequencies of axial vibration for Model A and B propulsion engine

Node	Without damping of A/V in Model A	With damping of A/V(as a de-tuner) in Model A	Without damping of A/V in Model B	With damping of A/V(as a de-tuner) in Model B
0	266.74	346.85	234.46	397.27
1	566.60	576.80	655.19	821.86
2	826.72	914.93	935.29	955.34

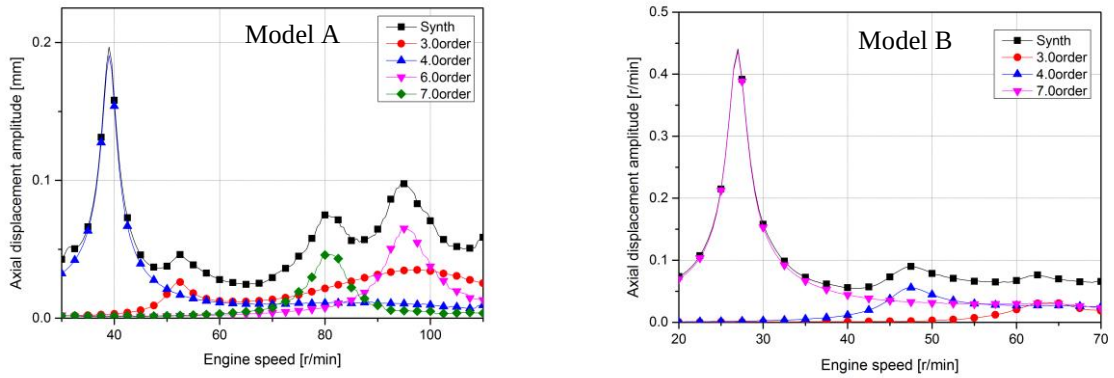

Figure 5: Axial displacement amplitude at thrust bearing

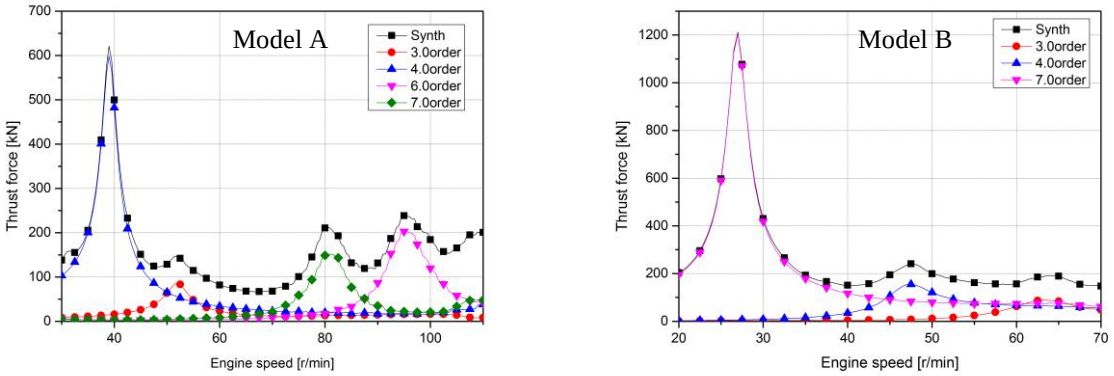

Figure 6: Thrust variation force at thrust bearing

The thrust variation force is shown in Fig. 6. For model A, the axial vibration and the torsional vibration was identified to be at 4th order component and the first node 4th order component of the resonance point 40 r/min. This can be regarded as a torsional-to-longitudinal vibration caused by the thrust variation force generated on the propeller shaft and the excitation force on the crankshaft due to the large torsional vibration. In model B, the thrust variation force was identified at the 7th order component and the resonance peak due to the torsional vibration is around 27 r/min.

In addition, the longitudinal vibration in Fig. 6 is the thrust force on the thrust bearing. This acts as the exciting force and is being transmitted to cause the longitudinal vibration in the upper part of the hull. In the case of the container ship, the axial vibration natural frequencies are identified to be between 350~400 cpm (cycle per minute) at the 4th order of the main resonance point. In this engine model, this phenomenon is not expected to occur.

4. Experiment Result

The equipment layout for comprehensive vibration measurement which includes axial vibration for the model marine diesel engines are shown in Fig. 7. The axial displacement and angular velocity was measured on the intermediate shaft nearest to the thrust bearing using gap sensor for Model A and LVDT for Model B. Figure 8 shows the axial displacement at crankshaft free end of the

model engines. The axial displacement amplitude was found to be at the 4th order around 0.35 mm and the 7th order around 0.12 mm at the resonance point of Model A and Model B engines respectively. These values did not deviate greatly from the theoretical calculation of the axial displacement at crankshaft free end being around 0.27 mm at 4th order and 0.20 mm at 7th order. On Fig. 9 Model A, the dominant 4th order thrust block axial displacement amplitude from Fig.5 Model A theoretical calculation was not detected through the actual vibration measurement. As such, the thrust variation force cannot be calculated through actual vibration measurement data. In addition, the 1st order and 2nd order axial displacement amplitude can be assumed to be due to the engine run-out and shaft misalignment of Model A engine respectively. Likewise, the 6th order zero-node thrust block amplitude near the mcr is attributed to the axial vibration first node effect yet the value is almost negligible. Here, even the thrust force occurs due to larger propeller skew and rake angle design, it is not directly translated to the crankshaft but rather up to the thrust block only and this amplitude can be assumed as a result of translated motion of the shafting system. On the other hand, the thrust block axial displacement of Fig.9 Model B was measured to be around 0.45 mm at 7th order of the resonance point. Figure 10 shows the actual measurement thrust variation force calculation of engine Model B to be around 1250 kN and this value does not differ with the theoretical calculation value of 1200 kN in Fig. 6 Model B.

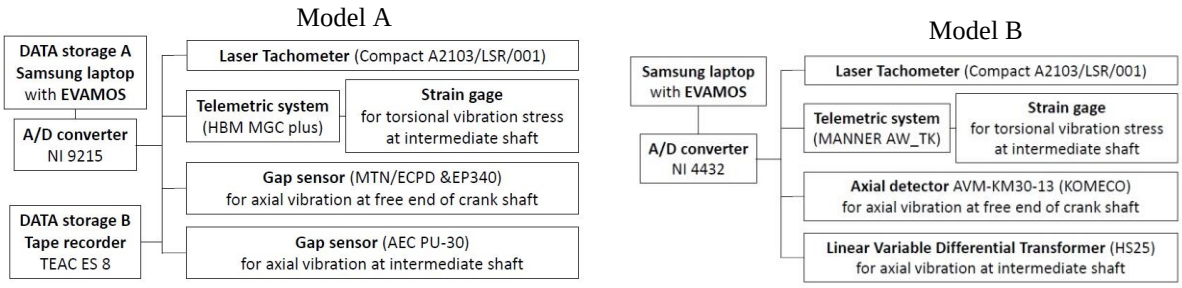

Figure 7: Schematic diagram for torsional and axial vibration measurement

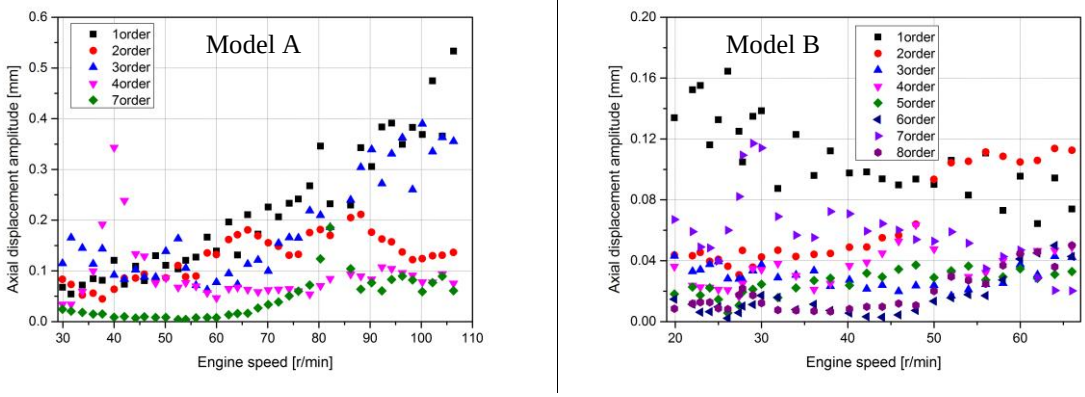

Figure 8: Crankshaft free end axial amplitude in normal firing condition

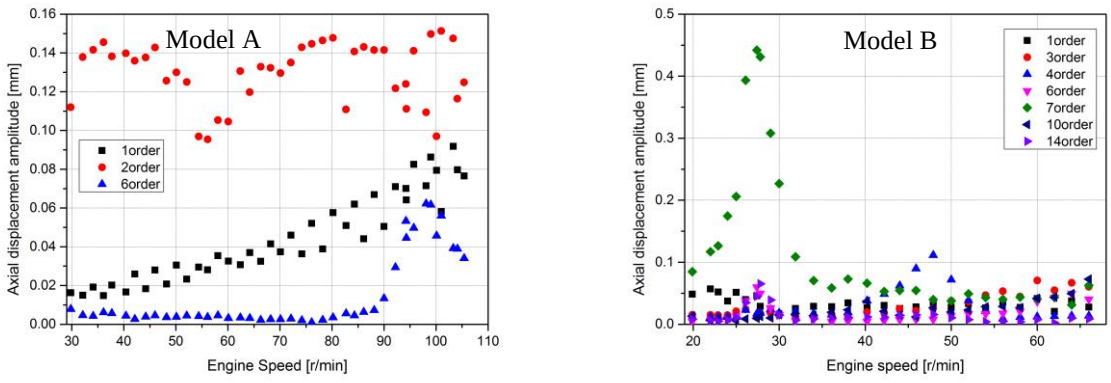

Figure 9: Thrust block axial displacement amplitude in normal firing condition

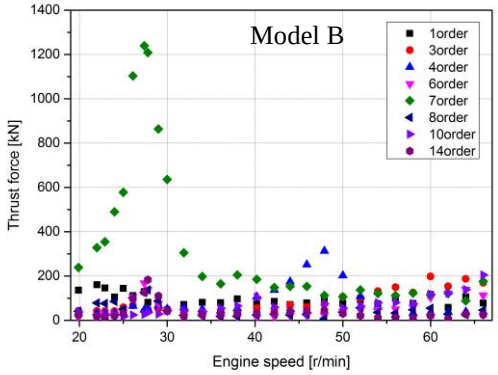

Figure 10: Thrust variation force based on measured axial displacement of intermediate shaft

These actual vibration measurement calculations verified the thrust variation force due to the coupled torsional and axial vibration influence on the dynamic behavior of the propulsion shafting system. However, it is presumed that considering the longer crankshaft length of Model A engine, the propeller does not affect the coupled torsional – axial vibration phenomenon of the propulsion shafting system. Further, although the trend and the magnitude did not differ greatly between the theoretical and actual measurement calculation, it confirmed that axial vibration has many complications in the damping and excitation force models as well as vibration model yielding large analysis and measurement deviations. However, even if the amplitude increases as long as the axial damper is active, there will be no problem protecting the crankshaft.

5. Conclusions

In this paper, the dynamic characteristics of axial vibration for an 80,080 kW 14RT-flex96C engine and a 24,400 kW 7G80ME super-long stroke engine were investigated through theoretical analysis and measurement.

1. Although the coupled torsional-axial vibration analysis and measurement results have been widely used, more practical results were obtained by considering the torsional vibration analysis as a significant vibration force for longitudinal vibration analysis in this study.
2. In the axial vibration measurement, the peak vibration amplitude is verified whether the axial vibration damper is working. However, it is necessary to confirm the thrust force variation since the thrust force due to torsional vibration is larger compared to mere longitudinal vibration and has a large influence on hull vibration.
3. For the axial vibration calculation of low-speed two-stroke diesel engine, straightforward modelling and excitation force are simply applied. However, additional modeling-based techniques and excitation force application methods should be further investigated and deemed necessary to define more accurate results.

REFERENCES

1 Fujii K. and Tanida K., *Exciting Forces of Ship Vibration Induced by Torsional and Longitudinal Vibration of Shafting System*, ICMES'84 (1984).

2 Hylarides S. and Gent van W., *Hydro dynamic Reactions to Propeller Vibrations*, Trans. I Mar E(C), Vol.91, Conference No.4, Paper C37. (1979).

3 Lee, D. C., Nam, J. G. and Ko, J. Y., *A Study of Axial Vibration of Two Stroke Low Speed Diesel Engine on the Diesel Power Plant*, Journal of the Korean Society for Noise and Vibration Engineering, Vol. 11 No. 9, pp.398~405,(2001).